Published in final edited form as:
Free Radic Biol Med. 2013 August ; 0: 298–309. doi:10.1016/j.freeradbiomed.2013.04.006.

Sites of superoxide and hydrogen peroxide production during fatty acid oxidation in rat skeletal muscle mitochondria

Irina V. Perevoshchikova[*], **Casey L. Quinlan**, **Adam L. Orr**, **Akos A. Gerencser**, and **Martin D. Brand**
Buck Institute for Research on Aging, Novato, CA 94945, USA

Abstract

H_2O_2 production by skeletal muscle mitochondria oxidizing palmitoylcarnitine was examined under two conditions: the absence of respiratory chain inhibitors and the presence of myxothiazol to inhibit complex III. Without inhibitors, respiration and H_2O_2 production were low unless carnitine or malate was added to limit acetyl-CoA accumulation. With palmitoylcarnitine alone, H_2O_2 production was dominated by complex II (44% from site II_F in the forward reaction); the remainder was mostly from complex I (34%, superoxide from site I_F). With added carnitine, H_2O_2 production was about equally shared between complexes I, II, and III. With added malate, it was 75% from complex III (superoxide from site III_{Qo}) and 25% from site I_F. Thus complex II (site II_F in the forward reaction) is a major source of H_2O_2 production during oxidation of palmitoylcarnitine ± carnitine. Under the second condition (myxothiazol present to keep ubiquinone reduced), the rates of H_2O_2 production were highest in the presence of palmitoylcarnitine ± carnitine and were dominated by complex II (site II_F in the reverse reaction). About half the rest was from site I_F, but a significant portion, ~40 pmol $H_2O_2 \cdot min^{-1} \cdot$ mg protein^{-1}, was not from complex I, II, or III and was attributed to the proteins of β-oxidation (electron-transferring flavoprotein (ETF) and ETF-ubiquinone oxidoreductase). The maximum rate from the ETF system was ~200 pmol $H_2O_2 \cdot min^{-1}$ ~ mg protein^{-1} under conditions of compromised antioxidant defense and reduced ubiqui-none pool. Thus complex II and the ETF system both contribute to H_2O_2 production during fatty acid oxidation under appropriate conditions.

Keywords

Palmitate; Palmitoylcarnitine; ROS; Complex I; Complex II; Succinate dehydrogenase; Complex III; ETF; Electron-transferring flavoprotein; ETFQOR; Electron transferring flavoprotein–ubiquinone oxidoreductase; Free radicals

Fatty acid β-oxidation by skeletal muscle mitochondria is a major source of ATP under physiological conditions [1,2], and impaired lipid metabolism is associated with several pathological conditions, such as multi-acyl-CoA dehydrogenase deficiency, obesity-related

[*]Corresponding author. irper@buckinstitute.org (I.V. Perevoshchikova).

insulin resistance, and type 2 diabetes [3]. Changes in reactive oxygen species (ROS)[1] production in these pathological conditions have been reported [4–8].

Palmitoylcarnitine is a major substrate for β-oxidation. It enters mitochondria on the carnitine–acylcarnitine translocase and is converted to palmitoyl-CoA. The fatty acid β-oxidation spiral involves four sequential enzymes: acyl-CoA dehydrogenase, 2-enoyl-CoA hydratase, L-3-hydroxyacyl-CoA dehydrogenase, and 3-ketoacyl-CoA thiolase [9]. In contrast to peroxisomal β-oxidation, in which molecular oxygen serves as the electron acceptor of acyl-CoA oxidases, mitochondrial acyl-CoA dehydrogenases transfer single electrons to electron-transferring flavoprotein (ETF) [10]. Singly reduced ETF^{-} is then oxidized by ETF-ubiquinone oxido-reductase (ETFQOR), which donates electrons directly to the ubiquinone (Q) pool in the mitochondrial inner membrane [11–13], to be passed to complex III of the respiratory chain, cytochrome *c*, complex IV, and finally molecular oxygen. The second dehydrogenation reaction in the β-oxidation spiral is catalyzed by hydroxyacyl-CoA dehydrogenase, which uses NAD^{+} as its electron acceptor. The reduced NADH is then oxidized by complex I, reducing the Q pool. The end product of β-oxidation, acetyl-CoA, condenses with oxaloacetate to form citrate, which is then oxidized by the Krebs cycle. Thus fatty acid oxidation in mitochondria is linked to oxidative phosphorylation and ATP production.

In contrast to many other substrates, such as malate, glutamate, succinate, or glycerol 3-phosphate, oxidation of fatty acids requires four enzymatic reactions and donates electrons at multiple points in the electron transport chain: complex I, ETFQOR, and complex II (via formation of succinate in the Krebs cycle). This makes fatty acid oxidation a good candidate for high rates of superoxide or H_2O_2 formation due to possible leaks of electrons to molecular oxygen at several different sites.

There are several sites of superoxide or H_2O_2 production in the Krebs cycle and electron transport chain [14–16]. In order of maximum capacity in skeletal muscle mitochondria, they are the ubiquinol-oxidizing site of complex III (site III_{Qo}), the ubiquinone-reducing site of complex I (site I_Q) and the flavin site of complex II (site II_F), the flavin site of complex I (site I_F), and the Q-binding site of glycerol 3-phosphate dehydrogenase (GPDH) [17,18]. Other sites include the dihydrolipoate moieties of 2-oxoglutarate dehydrogenase and pyruvate dehydrogenase, and the ETF/ETFQOR system, but their maximum rates have not been established. The native rates from various sites in the absence of inhibitors have been measured only during oxidation of glutamate and malate, when sites I_F and III_{Qo} dominate [19]; oxidation of succinate, when site I_Q dominates [20,21]; and oxidation of glycerol 3-phosphate, when site I_Q dominates and sites II_F and GPDH also contribute [17,18].

The sites of H_2O_2 production during oxidation of palmitoylcarnitine by skeletal muscle mitochondria have been addressed in earlier studies in isolated mitochondria [20,22–25]. Although mitochondria isolated from the complex cellular environment lose some inputs of metabolic control, this widely used model still provides a detailed understanding of mechanisms of metabolic regulation, including those related to mitochondrial ROS production. These insights then feed forward our understanding of more complex systems such as intact cells, tissues, or animals. Prior studies in isolated mitochondria have identified

several different components of the respiratory chain and β-oxidation pathway as sources of H_2O_2 during palmitoylcarnitine oxidation by isolated mitochondria: site I_Q [20,23], site III_{Qo} [20,22–24], ETF/ETFQOR [20,22–24], and acyl-CoA dehydrogenase [22,25]. One possible source of disagreement is the use of site-specific inhibitors of the respiratory chain. Such inhibitors are great tools for understanding the capacities and mechanisms of H_2O_2 production at sites of interest. However, inhibition of one center disrupts normal electron flow and may lead to changes in the reduction states of other centers far from the site of inhibition, with consequent changes in their production of superoxide or H_2O_2. In the presence of inhibitors it becomes impossible to measure changes in native rates of H_2O_2 production in different metabolic states or disease models, which is crucial for the investigation of ROS-related physiology and pathology. Therefore it is of high importance to resolve the contradicting conclusions and perform measurements in the absence of respiratory chain inhibitors (native rates) that more closely match physiological conditions in vivo.

The disadvantages of site-specific inhibitors can be partially avoided by using endogenous reporters to predict rates of superoxide formation from sites I_F and III_{Qo}[19]. This approach assumes a unique relationship between the reduction state of the superoxide-producing species within the site and its rate of reaction with oxygen to generate superoxide (or H_2O_2). The reduction state of the superoxide producer can be detected by measuring the reduction state of an endogenous “reporter,” a species that is close to equilibrium with the superoxide-producing moiety. NADH was established as a reporter of rates of superoxide production at site I_F (plus any other sites that respond to NADH reduction state) and cytochrome b_{566} as a reporter of superoxide production at site III_{Qo}[19].

For the first time we provide a complete analysis and dissection of the specific sites of superoxide/H_2O_2 production during fatty acid oxidation in the absence of respiratory chain inhibitors. We also investigate the contribution of the ETF/ETFQOR system to the rates of H_2O_2 production in the absence and presence of complex III inhibitors that lead to reduction of the Q pool and estimate the maximum rate of H_2O_2 production from this system in skeletal muscle mitochondria. We identify complex II as a new site of superoxide and/or H_2O_2 production that was not recognized in earlier studies and whose H_2O_2 production was previously wrongly attributed to other sites.

Experimental procedures

Animals, reagents, and mitochondrial preparation

Female Wistar rats (Harlan Laboratories), age 5–8 weeks, were fed chow ad libitum with free access to water. Skeletal muscle mitochondria were isolated in Chappell–Perry buffer (100 mM KCl, 50 mM Tris, 2 mM EGTA, pH 7.1 at 25 °C) by standard procedures [26]. Protein concentration was determined by the biuret method. The animal protocol was approved by the Buck Institute Animal Care and Use Committee, in accordance with IACUC standards. All reagents were from Sigma (St. Louis, MO, USA) except for Amplex UltraRed (Invitrogen, Carlsbad, CA, USA) and atpenin A5 (Santa Cruz Biotechnology, Santa Cruz, CA, USA). The L-isomer of palmitoylcarnitine was used in all experiments.

H_2O_2 production

Rates of superoxide production were measured indirectly as rates of H_2O_2 production after conversion of superoxide to H_2O_2 by endogenous superoxide dismutase (SOD) in the matrix. H_2O_2 was detected using horseradish peroxidase oxidizing Amplex UltraRed to its fluorescent resorufin product [19,27]. Exogenous SOD was added to convert any superoxide released in the medium. Mitochondria (0.3 mg protein · ml^{-1}) were suspended in a medium containing 120 mM KCl, 5 mM Hepes, 5 mM K_2HPO_4, 1 mM EGTA, and 0.3% (w/v) bovine serum albumin (pH 7.0 at 37 °C), together with 5 U · ml^{-1} horseradish peroxidase, 25 U · ml^{-1} SOD, and 50 μM Amplex UltraRed. The fluorescence signal was recorded using a Varian Cary Eclipse spectrofluorimeter (λ_{ex}560 nm, λ_{em}590 nm) with constant stirring. Rates of fluorescence change were calibrated with known amounts of H_2O_2 and normalized to the amount of protein [27]. The rates of H_2O_2 production in the calibration curve in Fig. 6B (see below) were obtained by titrating rotenone in the presence of 4 μM FCCP and 5 mM malate [28].

NAD(P) reduction state

Experiments were performed using 0.3 mg mitochondrial protein · ml^{-1} at 37 °C in the same medium as for H_2O_2 measurements. The reduction state of endogenous NAD(P) was determined by autofluorescence [28] using a Shimadzu RF5301-PC spectrofluorimeter at λ_{ex} 365 nm, λ_{em} 450 nm. NAD(P) was assumed to be 0% reduced after 5 min without added substrate and 100% reduced with 5 mM malate and 4 μM rotenone (Fig. 2A). Intermediate values were determined as %NAD(P)H relative to the 0 and 100% values. Although this technique measures contribution from both mitochondrial NADH and mitochondrial NADPH, the content of NAD^+ plus NADH in skeletal muscle mitochondria is much greater than the combined $NADP^+$ and NADPH [28,29]. Moreover the enhancement of NADH fluorescence in mitochondria is two- to fourfold greater than it is for mitochondrial NADPH [30]. The higher content and greater fluorescence enhancement of NADH make the autofluorescence signal predominantly a measure of NADH. The $NAD(P)^+$ reduction states in the calibration curve in Fig. 6B (see below) were manipulated by varying the concentration of rotenone in the presence of 5 mM malate and 4 μM FCCP [28].

Cytochrome b_{566} reduction state

Experiments were performed at 1.5 mg mitochondrial protein · ml^{-1} in the same medium as for H_2O_2 measurements. The reduction state of endogenous cytochrome b_{566} was measured with constant stirring at 37 °C in an Olis DW-2 dual-wavelength spectrophotometer as $A_{566\ nm}$–$A_{575\ nm}$ [27]. The signal at this wavelength pair reports ~75% cytochrome b_{566} and ~25% cytochrome b_{562} [27,31]. Cytochrome b_{566} was assumed to be 0% reduced after 5 min without added substrate and 100% reduced with 5 mM succinate and 4 μM rotenone or with 15 μM palmitoylcarnitine plus 5 mM malate, both in the presence of 2 μM antimycin A (Fig. 2B, see below). Intermediate values were determined as %b_{566} reduced relative to the 0 and 100% values. At least 15 data points were used to calculate the average percentage reduction under each condition.

Respiration

Experiments were performed in the same medium as H_2O_2 measurements at 0.3 mg mitochondrial protein · ml^{-1}. Oxygen consumption was recorded at 37 °C using a Clark electrode. State 2 respiration was in the presence of substrates only. Phosphorylating (State 3) respiration was initiated by addition of 0.5 mM ADP. Nonphosphorylating (State 4) respiration was recorded after addition of 1 μg · ml^{-1} oligomycin and uncoupled respiration was measured after subsequent addition of 1 μM FCCP.

Complex II activity

Experiments were performed strictly as in [17] but with the buffer used in the present study. Activity was measured as the rate of reduction of 50 μM dichlorophenolindophenol (DCPIP) in the presence of 1 mM phenazine methosulfate instigated by addition of 10 mM succinate at 15 °C to freeze the activation state.

Endogenous reporters of superoxide production

The method is described in [19]. Briefly, the reduction state of $NAD(P)^+$ was used to predict superoxide production from site I_F from the calibration curve in Fig. 2A (inset, see below) for all data except Figs. 6C and 7 (ETF/ETFQOR system), which used the calibration in Fig. 6B (see below). The reduction state of cytochrome b_{566} was used to predict superoxide production from site III_{Qo} using the calibration curve in Fig. 2B (inset, see below).

Statistics and curve fitting

Data are presented as means ± SEM. Differences between groups were assessed by Student's *t* test using SigmaPlot version 11. One-way ANOVA was used to compare differences in H_2O_2 production after antimycin A treatment (Fig. 4A and B). Calibration curves in Fig. 2A and B were single exponential fits [19]. The calibration curve in Fig. 6B was fit poorly by a single exponential, so it was fitted empirically using Eq. (1), which assumes that the reporter (NADH) and the superoxide producer ($FADH_2$) have different potentials but are close to equilibrium:

$$\ln\left(\frac{100-\frac{y}{k}}{\frac{y}{k}}\right)=a+\frac{1}{2}\ln\left(\frac{100-x}{x}\right), \quad (1)$$

where *y* is the rate of H_2O_2 production (pmol · min^{-1} · mg $protein^{-1}$); *x* is the reduction state of the NAD^+ pool (% NAD(P)H); k=0.0033 · pmol · $\%^{-1}$ · min^{-1} · mg $protein^{-1}$, a scaling factor expressing the rate constant of H_2O_2 formation; and a = 2.05, a parameter proportional to the difference in midpoint potentials. The errors caused by the calibrations were calculated for each *x* value as the root mean square of the linearly interpolated SEM of the *x* value propagated through the calibration equation and linearly interpolated SEM of the *y* value.

Errors for predicted rates of H_2O_2 production (Figs. 3, 5B, 5C, and 6C) were calculated as the root mean square of the calibration errors above and the propagated SEMs of the reporter level through the calibration equation. Exact equations are in [19]. Welch's *t* test was used to compare measured and predicted values in Figs. 3, 5B, 5C, and 6C.

Results

Oxygen consumption by skeletal muscle mitochondria oxidizing palmitoylcarnitine

Table 1 summarizes the respiration rates of mitochondria on succinate plus rotenone and on three substrate combinations commonly used to assess β-oxidation. Respiration on succinate had appropriate high rates and respiratory control. Palmitoylcarnitine alone supported very slow respiration that was not stimulated by ADP or uncoupler, presumably because 3-ketoacyl thiolase, the last reaction of β-oxidation, was limited by the high acetyl-CoA/CoA ratio [32].

Addition of carnitine rescues this condition by accepting acetyl groups from acetyl-CoA to generate acetylcarnitine and CoA in a reaction catalyzed by carnitine acetyltransferase. The acetylcarnitine is then exported in exchange for incoming carnitine. Carnitine acetyltransferase activity is much higher in mitochondria from skeletal muscle (410 μmol · min^{-1} · mg $protein^{-1}$) than from liver (5 μmol · min^{-1} · mg $protein^{-1}$) [33], and there is correspondingly increased respiration on palmitoylcarnitine after addition of carnitine in mitochondria from skeletal muscle but not liver [24]. Table 1 shows that inclusion of carnitine stimulated oxidation of palmitoylcarnitine sufficiently to allow respiratory control. The combination of palmitoylcarnitine plus carnitine was attractive for this study because its metabolism may generate H_2O_2 without overt involvement of Krebs cycle enzymes.

Addition of malate also rescues oxidation of palmitoylcarnitine, by generating oxaloacetate through malate dehydrogenase. Citrate synthase then condenses oxaloacetate and acetyl-CoA to form citrate, releasing CoA. Table 1 shows that palmitoylcarnitine plus malate supported substantial phosphorylating and uncoupled respiration and good respiratory control.

Thus, oxidation of palmitoylcarnitine, supplemented by either carnitine or malate, provides sufficient electron flux to establish these physiologically relevant substrate combinations as suitable for further investigation.

H_2O_2 production during oxidation of palmitoylcarnitine in the absence of respiratory chain inhibitors

Fig. 1A shows that addition of palmitoylcarnitine at 5 min caused a measureable increase in the rate of Amplex UltraRed oxidation to resorufin; this was subsequently calibrated by additions of H_2O_2 to give the rate of H_2O_2 production. The open bars in Fig. 1B show the overall rates of H_2O_2 production measured in this way during oxidation of each of the fatty acid substrate combinations in Table 1. Oxidation of palmitoylcarnitine alone produced H_2O_2 at a low rate. Addition of malate or carnitine increased the rate several fold. The maximum rate was found with palmitoylcarnitine plus carnitine.

Next, we determined the individual sites of H_2O_2 production with these substrate combinations. Even though respiration on palmitoylcarnitine alone was slow, we included it because, surprisingly, site II_F of complex II was the major H_2O_2 producer under this condition (Figs. 3 and 5B below).

Complex II generates superoxide and/or H_2O_2 in the forward reaction during palmitoylcarnitine oxidation in the absence of respiratory inhibitors

Addition of malonate, a specific inhibitor of succinate oxidation, significantly decreased the rates of H_2O_2 production with palmitoylcarnitine (Fig. 1A and B) and with palmitoylcarnitine plus carnitine, but had little effect on the rate with palmitoylcarnitine plus malate (Fig. 1B, shaded bars). These observations can be explained by generation of superoxide or H_2O_2 at complex II, which is sensitive to malonate during oxidation of succinate or glycerol3-phosphate in the presence of rotenone (to inhibit complex I) and myxothiazol (to inhibit complex III) in skeletal muscle mitochondria [17,18]. Malonate sensitivity of H_2O_2production during oxidation of palmitoylcarnitine has not been described before and is explored in more detail below.

We propose that under these conditions addition of palmitoylcarnitine (±carnitine) triggers superoxide or H_2O_2 production from site II_F using electrons from endogenous succinate, but addition of palmitoylcarnitine plus malate does not. This hypothesis is supported by several observations.

First, measurements of complex II activity showed that palmitoylcarnitine± carnitine indirectly activated the enzyme, explaining the trigger mechanism. To calibrate, incubation of mitochondria with 5 mM succinate plus rotenone and myxothiazol at 37 °C gave high complex II activity (80±6 nmol DCPIP $\cdot$ min^{-1} $\cdot$ mg $\cdot$ $protein^{-1}$), and incubation without succinate gave low activity (40±4 units). Incubation with palmitoylcarnitine alone without rotenone or myxothiazol gave an activity of 64±8 units and incubation with palmitoylcarnitine plus carnitine gavean activity of 61±8 units (all values mean±SEM, *n*=3). This substantial activation of complex II by palmitoylcarnitine can be explained by removal of inhibitory oxaloacetate by condensation with acetyl-CoA formed by β-oxidation. In contrast, malate oxidation produces excess inhibitory oxaloacetate and prevented superoxide and/or H_2O_2 production from site II_F when palmitoylcarnitine plus malate was used as substrate.

Second, atpenin A5, an inhibitor of the ubiquinone binding site of complex II [34], did not prevent H_2O_2 production with palmitoylcarnitine as substrate, but stimulated it. It is known that H_2O_2 production from site II_F in the forward reaction from succinate is not prevented byatpenin A5 (unlike the reverse reaction from Q), but instead is stimulated as the flavin of complex II becomes more reduced [17]. Fig. 1A shows that addition of atpenin A5 increased the rate of H_2O_2 production in the presence of palmitoylcarnitine alone, whereas malonate decreased the rate. The stimulated rate in the presence of atpenin A5 was abolished by subsequent addition of malonate (Fig. 1A), showing that it emanated from site II_F operating in the forward reaction from succinate (because the reverse reaction from QH_2 was inhibited by atpenin A5). The stimulation of H_2O_2 production by subsequent addition of myxothiazol is addressed below (Fig. 5). Therefore, malonate but not atpenin A5 was used under native conditions below to inhibit H_2O_2 production from site II_F.

We conclude from Fig. 1 that site II_F in the forward reaction produced ~25% of the observed H_2O_2 during oxidation of palmitoylcarnitine plus carnitine and ~75% during oxidation of palmitoylcarnitine alone. When malate was present and the substrate-binding site of

complex II was inhibited by oxaloacetate, oxidation of palmitoylcarnitine did not result in significant H_2O_2 production from site II_F. After correction for small changes in H_2O_2 production from sites I_F and III_{Qo} after addition of malonate (see Fig. 3 below), the contribution of site II_F become 36% for palmitoylcarnitine plus carnitine and 44% for palmitoylcarnitine alone.

Quantitative contributions of sites I_F, III_{Qo}, and II_F to superoxide and/or H_2O_2 production during oxidation of palmitoylcarnitine

Endogenous reporters can predict the rates of superoxide production from sites I_F and III_{Qo} in the absence of site-specific respiratory inhibitors (e.g., rotenone, antimycin A, myxothiazol, or stigmatellin) [19]. We used this technique in this work. We measured the reduction state of endogenous NAD(P) (Fig. 2A), to report superoxide production from site I_F (plus any other sites that respond to NADH reduction state), and cytochrome b_{566} (Fig. 2B), to report superoxide production from site III_{Qo}. The corresponding calibration curves are shown as insets in Fig. 2A and B. Table 2 presents the reduction states of NAD(P) and cytochrome b_{566}under the conditions of Fig. 1B and the rates of H_2O_2 production from sites I_F and III_{Qo} predicted from the calibration curves.

The effect of malonate addition on the reduction of the reporters and the predicted rates of H_2O_2 production is also presented in Table 2. Malonate had no discernible effect on the predicted rate from site I_F, but it lowered the predicted rate from site III_{Qo} with palmitoylcarnitine alone and raised it with palmitoylcarnitine plus carnitine (although these effects were not statistically significant). These data allowed the raw decrease in H_2O_2 production rate at site II_F caused by addition of malonate (Fig. 1B) to be corrected for consequent changes in H_2O_2 production rate at sites I_F and III_{Qo}. The corrected values for site II_F are shown in Table 2.

For each substrate combination, Fig. 3 shows the predicted rates of H_2O_2 production from sites I_F, III_{Qo}, and II_F from Table 2 (black, gray, and striped bars) and compares them to the empirical rates (open bars) from Fig. 1B. During oxidation of palmitoylcarnitine alone, site II_F was the dominant site, responsible for 44% of the total predicted rate of H_2O_2 production. Site I_F produced 34% and site III_{Qo} produced 22% of the total predicted rate. When palmitoylcarnitine was oxidized with carnitine supplementation, the contributions from sites I_F (29%), III_{Qo} (35%), and II_F (36%) were approximately equal. When palmitoylcarnitine plus malate was used as substrate, site II_F did not contribute (because it was inhibited by the added malate). Site III_{Qo} was the major superoxide producer (75%), with the remaining 25% contributed by site I_F.

In each case, the predicted rates fully accounted within experimental error for the empirical rates, demonstrating that essentially all the H_2O_2 produced during oxidation of palmitoylcarnitine in the absence of respiratory chain inhibitors came from these three sites, and any contribution from other sites was below the detection limit of this methodology.

Thus, we have identified and quantified the native sites of superoxide or H_2O_2 production during fatty acid oxidation by rat skeletal muscle mitochondria in the absence of respiratory chain inhibitors and absence of ATP synthesis. Site II_F of complex II was identified as one

of the major contributors. The ETF/ETFQOR system, other enzymes of the β-oxidation spiral, and site I_Q were not shown to be major sources of H_2O_2 under any condition examined, because there were no significant differences between the observed rates and the sum of the rates predicted by the endogenous reporters or prevented by inhibition of site II_F.

Rates of H_2O_2 production with palmitoylcarnitine plus antimycin A

We now switch from conditions with the Q pool relatively oxidized to studies with complex III inhibited to keep the QH_2/Q ratio high. This condition was used in earlier studies and revealed very high rates of H_2O_2 production from unknown sites. It was proposed to originate from complexes upstream of the Q pool such as ETF, ETFQOR, and acyl-CoA dehydrogenase [20,22,24]. We did not find that these enzymes produced measureable superoxide or H_2O_2 in the absence of respiratory inhibitors (above). Here we explore if reduction of the Q pool can cause high rates of H_2O_2 production from these or other upstream centers to reveal the mechanism of superoxide and/or H_2O_2 production from fatty acid oxidation-specific enzymes.

Fig. 4A shows that addition of antimycin A, an inhibitor of the Q_i site of complex III, caused very rapid H_2O_2 production with palmitoylcarnitine plus carnitine as substrate. Rates with palmitoylcarnitine alone were similar, but rates with palmitoylcarnitine plus malate were lower (Fig. 4B, open bars).

We estimated the contributions of sites III_{Qo} and II_F in each case. Antimycin A inhibition of the Q_i site enhances superoxide production from site III_{Qo}, which is prevented by Q_o site inhibitors, including myxothiazol [27,35–37]. Fig. 4 shows that addition of myxothiazol strongly inhibited H_2O_2 production with all three substrate combinations, showing that site III_{Qo} was a major contributor under these conditions, as expected. However, with palmitoylcarnitine ± carnitine, myxothiazol inhibition was incomplete, suggesting that sites other than III_{Qo} were also generating H_2O_2. The contribution of site II_F to the residual rates was estimated by adding malonate. This largely abolished H_2O_2 production (Fig. 4), suggesting that most of the myxothiazol-insensitive rate originated not from the ETF system but from complex II.

Thus, the majority of H_2O_2 production by muscle mitochondria incubated with palmitoylcarnitine ± carnitine in the presence of antimycin A arose from sites III_{Qo} and II_F. The important contribution from site II_F explains why there was a lower overall rate and a greater proportional contribution from site III_{Qo} in the presence of malate (Fig. 4B): malate completely inhibited this contribution of site II_F.

To quantify fully the contributions of each site in the presence of antimycin A, any effects of myxothiazol and malonate on the reduction state of site I_F should be measured using the changes in NAD(P)H and corrected for, as in Table 2 and Fig. 3 (complex III stays fully reduced under these conditions, so its contribution to the signal does not change when malonate is added). Unfortunately, the strong fluorescence of antimycin A at 450 nm overlaps NAD(P)H autofluorescence, making it hard to correct for changes at site I_F accurately with antimycin A present. Therefore, we used myxothiazol alone in all following experiments.

Rates of H_2O_2 production with palmitoylcarnitine plus myxothiazol

Fig. 5 shows the rates of H_2O_2 production with myxothiazol alone (to prevent superoxide formation at site III_{Qo} yet still allow correction for any changes in superoxide production at site I_F after addition of inhibitors). These rates were slower than those with antimycin A plus myxothiazol (Fig. 4), which can be explained by more complete inhibition of complex III and higher QH_2/Q ratio when both inhibitors were present. Addition of malonate very strongly inhibited the rates with palmitoylcarnitine ± carnitine, but not with palmitoylcarnitine plus malate. Measurement of $NAD(P)^+$ reduction state allowed prediction of the rates from site I_F under each condition using the calibration curve in Fig. 2A (inset) and correction of the rates from site II_F for the small changes in the rate from site I_F on addition of malonate.

Fig. 5B reports the contributions of sites I_F and II_F to H_2O_2 production in the presence of myxothiazol. With palmitoylcarnitine± carnitine, H_2O_2 production was dominated by site II_F, which accounted for ~70% of the total measured rates. Site I_F produced only a small amount,~4% of the totals. When palmitoylcarnitine plus malate was used as substrate, site II_F did not contribute (because it was inhibited by the added malate), and site I_F was the major superoxide producer (68% of the total measured rate).

In the presence of myxothiazol, H_2O_2 production from site II_F with palmitoylcarnitine was depressed by addition of carnitine (Fig. 5B). This can be explained by a measured decrease in the activity of complex II from 58.2±6.1 to 45.6±6.5 nmol DCPIP min^{-1} mg $protein^{-1}$(*n*=3) under these conditions. This was presumably because decreased flux through the ETF pathway in the presence of myxothiazol stalled β-oxidation and lowered acetyl-CoA production, allowing removal of acetyl-CoA by carnitine and accumulation of inhibitory oxaloacetate.

From Fig. 1A we concluded that site II_F produced H_2O_2 in the forward reaction from succinate during palmitoylcarnitine oxidation under native conditions, because the rate was inhibited by malonate (which inhibits at the flavin site) but stimulated by atpenin A5 (which inhibits at the Q-binding site of complex II). However, the situation was different in the presence of antimycin A (Fig. 4A) or myxothiazol (Fig. 5A), when the Qpool was much more reduced. In each case, atpenin A5 inhibited H_2O_2 production as effectively as malonate, showing that under these conditions the route of electrons into site II_F was by the reverse reaction, from the Q pool.

Importantly, unlike the native condition (Fig. 3), in the presence of myxothiazol there was a clear and significant difference between the empirical rate and the sum of the predicted rates of H_2O_2 production, with palmitoylcarnitine plus either carnitine or malate as substrate (Fig. 5B). This H_2O_2 production was not from site I_F, I_Q, II_F, or III_{Qo}, because these sites were either accounted for or inhibited directly (or, for site I_Q, inhibited indirectly by abolishing proton-motive force).

To investigate this unassigned rate more closely, in Fig. 5C we analyzed the residual rate after myxothiazol addition when complex II was inhibited from the start of the experiment (i.e., malonate added together with substrate). This avoided errors introduced in correcting

for contributions from other sites and led to a more significant difference between the empirical and the predicted rates, even though NAD(P) was more reduced after myxothiazol addition (because the escape of electrons to complex II was prevented), and superoxide production from site I_F was increased (Fig. 5C).

Thus, complex II produces superoxide and/or H_2O_2 at very high rates by the reverse reaction at site II_F using electrons from the Q pool when mitochondria oxidize palmitoylcarnitine ± carnitine in the presence of antimycin A or myxothiazol. This novel finding has to be taken into account in interpreting other studies using fatty acids as substrate. In the presence of palmitoylcarnitine plus carnitine, malonate, and myxothiazol there was a highly significant rate of H_2O_2 production that was not accounted for by site I_F, I_Q, II_F, or III_{Qo} (Fig. 5C); we argue below that it originated in the ETF/ETFQOR system.

Maximum rate of H_2O_2 production by the putative ETF/ETFQOR system

We searched for conditions that maximized H_2O_2 production dependent on the presence of palmitoylcarnitine that was unattributed to characterized sites. High rates were obtained in the presence of the uncoupler FCCP. This approach had two benefits. (i) Uncoupling oxidized the electron transport chain and therefore enzymes involved in electron supply were not inhibited by their products. Subsequent addition of myxothiazol caused a strong reduction of the Q pool and upstream redox centers ($NAD(P)^+$, ETFQOR, ETF). (ii) Uncoupling compromised the antioxidant defense systems by decreasing NAD(P)H formation by energy-dependent transhydrogenase and reduction of the glutathione pool [38].

In uncoupled mitochondria respiring on palmitoylcarnitine plus carnitine in the presence of malonate to inhibit site II_F, myxothiazol addition caused a high initial rate of H_2O_2 production. This decreased to a lower rate after a few minutes (Fig. 6A). The possible mechanism of this biphasic kinetics is discussed below. Calculation of the contribution of site I_F required a calibration curve obtained under the same conditions as a compromised antioxidant defense system. Fig. 6B shows the dependence of H_2O_2 production from site I_F on NAD(P)+ reduction state in the presence of FCCP. The calibration curve superimposed that obtained after treatment of mitochondria with1-chloro-2,4-dintrobenzene (CDNB) to deplete glutathione [19], consistent with the interpretation that FCCP also compromised the glutathione pool.

Fig. 6C shows the empirical rates in the fast and slow phases and the predicted contributions of site I_F, the only characterized site that was active under these conditions. The final nonpredicted rate of H_2O_2 production in the fast phase was 210±11 pmol $\cdot$ min^{-1} $\cdot$ mg $protein^{-1}$, which probably originated from the ETF/ETFQOR system.

Fig. 7 compares the rate that we have assigned to ETF/ETFQOR to the maximum rates of superoxide/H_2O_2 production from the other characterized sites. The maximum rate from ETF/ETFQOR was much less than the maximum capacities of sites III_{Qo}, I_Q, and II_F, but comparable to the maximum capacities of site I_F and glycerol 3-phosphate dehydrogenase.

Discussion

We have characterized the rates and sites of origin of H_2O_2 production in isolated rat skeletal muscle mitochondria oxidizing substrates of β-oxidation under two conditions: the absence of respiratory inhibitors (Fig. 3) and with complex III inhibited to reduce the Q pool (Figs. 4 and 5B).

In contrast to previous studies of fatty acid oxidation (see the introduction) we used endogenous reporters in the absence of respiratory inhibitors to pinpoint sites of superoxide and/or H_2O_2 production under native conditions. We found that the flavin site of complex I (site I_F) (plus any other sites that respond to NADH reduction state) and the Q_o site of complex III (site III_{Qo}) produced much of the superoxide during oxidation of palmitoylcarnitine. For the first time, the flavin site of complex II (site II_F) was found to produce superoxide and/or H_2O_2 in the forward reaction at substantial rates during oxidation of palmitoylcarnitine ± carnitine (Fig. 3). There was no significant contribution by any other site.

With complex III inhibited using antimycin A, site III_{Qo} was the major site, and site II_F produced superoxide and/or H_2O_2 at a high rate in the reverse reaction from the reduced Q pool (unless it was inhibited by added malate; Fig. 4B). When complex III was inhibited by myxothiazol to eliminate site III_{Qo}, site II_F was dominant, with only a small contribution from site I_F (Fig. 5B). Another site, probably the ETF/ETFQOR system, contributed significantly to H_2O_2 production under these conditions, with a maximum rate of 210 pmol · min^{-1}· mg $protein^{-1}$under optimal conditions (Fig. 6C).

Now we will consider each site in turn:

Site I_F

Superoxide production by complex I (plus any other sites that respond to NADH reduction state) increases at higher NADH/NAD^+ ratio [19,28,39–41]. During β-oxidation, hydroxyacyl-CoA dehydrogenase converts one NAD^+ to NADH per turn of the cycle, making site I_F an appealing superoxide-producing candidate during fatty acid oxidation. However, oxidation of palmitoylcarnitine alone reduces NAD^+ to a much lower extent than that of NAD-linked substrates such as glutamate plus malate, so the contribution of site I_F has been thought to be negligible [24]. We found similar results (15% $NAD(P)^+$ reduction with palmitoylcarnitine (Table 2) and 85% $NAD(P)^+$ reduction with glutamate plus malate [19]), presumably because oxidation of palmitoylcarnitine was restricted by a high acetyl-CoA/CoA ratio, which inhibits the last enzyme of β-oxidation, 3-ketoacyl thiolase [32]. Nonetheless, Fig. 3 shows that site I_F was a major contributor to the low rate of superoxide production with palmitoylcarnitine alone as substrate.

Addition of carnitine or malate to mitochondria respiring on palmitoylcarnitine removes acetyl-CoA. This greatly increased NAD(P) reduction (Table 2) and thus superoxide production from site I_F. However, the relative contribution of site I_F was not much changed because of increased production at other sites as well (Fig. 3).

When complex III was inhibited, strong reduction of the Q pool caused other sites to increase superoxide or H_2O_2 production greatly, and the relative contribution of site I_F was correspondingly decreased (Figs. 4B, 5B, and 6C). However, when these other sites were inhibited by addition of myxothiazol and malate or malonate, site I_F was a major contributor to the remaining low rates (Figs. 5B and 5C).

Site I_Q

Superoxide is produced at site I_Q a thigh rates when the proton-motive force and pH gradient are large, both during reverse electron flow from a reduced Q pool during oxidation of succinate [21,42] or glycerol3-phosphate [17,18,43]and during forward electron flow from NADH in the presence of certain I_Q inhibitors [42,44]. Because oxidation of fatty acids can reduce NAD^+ through hydroxyacyl-CoA dehydrogenase and the Q pool through acyl-CoA dehydrogenase and maintain a high proton-motive force and pH gradient, it has been speculated that oxidation of fatty acids smaysupport superoxide production at site I_Q [20,23,42]. We found no evidence for production of superoxide at site I_Q during oxidation of fatty acids, because there was no significant rate unattributable to sites I_F, II_F, and III_{Qo} under native conditions (Fig. 3). In the presence of complex III inhibitors the proton-motive force will have collapsed, so site I_Q is not a candidate for the unattributed H_2O_2 production rates in Figs. 5B, C, and 6C. Our results do not support the hypothesis that fatty acid oxidation generates superoxide at site I_Q, in agreement with the conclusions of others [24,45].

Site III_{Qo}

Superoxide is produced during oxidation of QH_2 at the Q_o site of complex III [46,47] at a rate that depends on the QH_2/Q ratio [27]. During oxidation of fatty acids the Q pool can be reduced by complex I, complex II, and ETFQOR. Cytochrome b_{566}, which reports the reduction state of the Q pool [19,27], was more reduced with palmitoylcarnitine plus malate (48%; Table 2) than with glutamate plus malate (37%) [19], leading to high rates of superoxide production from site III_{Qo}. In this study superoxide production from III_{Qo} made the greatest individual contribution to total H_2O_2 production under native conditions with palmitoylcarnitine plus carnitine or malate (Fig. 3) and when complex III was inhibited by antimycin A (Fig. 4B). Its high contribution had to be eliminated by addition of myxothiazol to allow analysis of the smaller rates from the ETF/ETFQOR system (Figs. 5 and 6). Site III_{Qo} was also identified in previous studies using antimycin A [20,22–24].

Site II_F

This is the first report of H_2O_2 production from complex II during fatty acid oxidation. Under native conditions, inhibition by malonate was diagnostic of the contribution of complex II to the observed rate of H_2O_2 production (Fig. 1). Site II_F was a major contributor unless it was inhibited by addition of malate (Fig. 3). In contrast, the Q-binding-site inhibitor atpenin A5 increased H_2O_2 production with palmitoylcarnitine. This H_2O_2 production was abolished by subsequent addition of malonate (Fig. 1A), implicating forward electron flow into the flavin site of complex II. This effect can be explained by activation of complex II by the added palmitoylcarnitine generating acetyl-CoA and consuming endogenous inhibitory

oxaloacetate, allowing endogenous succinate to cause H_2O_2 production at site II_F in the forward reaction under our experimental conditions.

When complex III was inhibited, site II_F was a major contributor to the high observed rates of H_2O_2 production (Fig. 4B) and the dominant contributor when site III_{Qo} was inhibited by myxothiazol (Fig. 5B). Both malonate and atpenin A5 strongly inhibited myxothiazol-induced H_2O_2 production (Figs. 4 and 5A), strongly supporting the idea that complex II can produce superoxide and/or H_2O_2 at high rates in the reverse reaction from a reduced Q pool during fatty acid oxidation.

Other sites

When electron flow through complex III was abolished and sites I_F, I_Q, II_F, and III_{Qo} were inhibited or fully accounted for, there remained a significant rate of H_2O_2 production in the presence of palmitoylcarnitine plus carnitine or malate (Figs. 5B, 5C, and 6C). The possible candidates are other enzymes directly connected to the Q pool, including ETFQOR, glycerol 3-phosphate dehydrogenase, dihydroorotate dehydrogenase, sulfide ubiquinone oxidoreductase, and proline dehydrogenase, as well as enzymes of the Krebs cycle or β-oxidation, including pyruvate and 2-oxoglutarate dehydrogenases, ETF, and acyl-CoA dehydrogenase.

The best candidate for the unassigned H_2O_2 production is the ETF/ETFQOR system, for the following reasons. (i) There is a requirement for substrates of β-oxidation, and these will reduce ETF/ETFQOR but not the other candidates by forward electron flow. (ii) Most candidates that might use electrons from the Q pool are present at rather low concentrations in skeletal muscle mitochondria. This is not true for glycerol 3-phosphate dehydrogenase, but it is not known to use electrons from the Q pool to generate H_2O_2 in the absence of glycerol 3-phosphate [18], making its participation unlikely. Skeletal muscle energy metabolism relies on β-oxidation, and therefore muscle mitochondria have high expression of the appropriate enzymes [48–50]. There is relatively high expression of ETFQOR (about 7% of total FAD-containing enzymes in the mitochondrial inner membrane [48]) and a larger ETF pool (63 pmol · mg protein^{-1} in skeletal muscle compared to brain mitochondria, which contain only 9 pmol · mg protein^{-1} of ETF [49]). Altogether, flavoproteins of β-oxidation account for 80% of the total content of mitochondrial flavoenzymes [50]. (iii) Compared to other complexes in the respiratory chain (complex I [51,52], complex II [53], glycerol 3-phosphate dehydrogenase [54,55], and dihydroorotate dehydrogenase [56,57]), ETFQOR has the most positive redox potentials (+27 mV for FAD_{1e^-}/FAD_{ox} and +47 mV for $[FeS]^{2+}/[FeS]^{1+}$) [58,59]. Therefore it is thermodynamically favorable for a reduced Q pool to reduce ETFQOR and possibly ETF. (iv) Isolated ETFQOR is kinetically reversible [13] and submitochondrial particles catalyze the reduction of ETF by NADH and succinate under anaerobic conditions [60]. Thus ETFQOR can reduce ETF using electrons from the Qpool.

We now discuss the possible sites within the ETF/ETFQOR system.

Acyl-CoA dehydrogenase

Acyl-CoA dehydrogenases, in contrast to acyl-CoA oxidases, have low reactivity toward molecular oxygen [10], because of desolvation of the active site [61]. Moreover, the reduced medium-chain acyl-CoA dehydrogenase complexed with enoyl-CoA product is essentially devoid of oxygen reactivity [61,62]. Thus, acyl-CoA dehydrogenase is not a likely candidate.

ETF and ETFQOR

Identification of the species within the ETF/ETFQOR system that generates superoxide or H_2O_2 is challenging. We were unable to obtain the most potent known inhibitor of ETFQOR, 2-(3-methylpentyl)-4,6-dinitrophenol [63], to test this question directly.

We hypothesize that ETF is the site of superoxide and/or H_2O_2 production. Several observations support this hypothesis. (i) The one-electron reduction of ETF by acyl-CoA dehydrogenase is fast [12,64]. (ii) The half-reduced species of isolated ETF produces superoxide and H_2O_2 at high rates [4]. (iii) The redox couple FAD_{1e^-}/FAD_{ox} in ETF has a more negative redox potential (+4 mV [65]) than the FAD in ETFQOR (+27 mV, see above), making ETF the better reductant of oxygen to superoxide or H_2O_2. (iv) The crystal structure of ETFQOR predicts low reactivity towards oxygen at all redox centers. The hydrophobic Q-binding pocket of the enzyme allows Q to penetrate deeply. If electron transfer to Q involves semiquinone as a transient intermediate, the semiquinone is protected from molecular oxygen. The FAD and FeS clusters are deeply buried and therefore unlikely to be reactive [66].

The biphasic kinetics of H_2O_2 production in Fig. 6A are probably explained by semiflavin ETF^- being the source of superoxide and H_2O_2. As ETF gradually becomes reduced in the presence of a high QH_2/Q ratio, ETF^- builds up, causing high initial rates of H_2O_2 production. This is followed by an abrupt switch to a second phase of slower H_2O_2 production, probably caused by fully reduced flavin ETF^{2-} as the whole ETF pool becomes fully reduced by acyl-CoA dehydrogenase. Two-electron reduction of ETF may occur either by acyl-CoA dehydrogenase at a much lower rate [12,64] or by disproportionation catalyzed by ETFQOR [12,59]. However, further experiments are required to establish the superoxide/H_2O_2-producing species within the ETF/ETFQOR system.

Conclusions

We have identified multiple sites of H_2O_2 and/or superoxide production during fatty acid oxidation in isolated skeletal muscle mitochondria. We conclude that when the Q pool is fairly oxidized, fatty acid oxidation in nonphosphorylating mitochondria produces superoxide and/or H_2O_2 mainly at site I_F, site II_F in the forward reaction, and site III_{Qo}, and the contribution of ETF/ETFQOR is negligible. However, reduction of the Q pool by inhibition of complex III causes high rates of superoxide and/or H_2O_2 production from site III_{Qo}, site II_F in the reverse reaction, ETF/ETFQOR, and site I_F. The contribution of each of these sites to superoxide and H_2O_2 production in cells during fatty acid oxidation under physiological or pathological conditions remains to be determined.

The reduction state of the Q pool was found to be crucial for the identification of the sites and mechanisms of superoxide and/or H_2O_2 production in isolated skeletal muscle mitochondria. However, it is difficult to correlate our in vitro conditions with in vivo studies because of the limited number of in vivo measurements of the reduction state of the Q pool in relevant systems. Direct measurements of flash-frozen samples of spontaneously contracting atria indicate that the Q pool is 40% oxidized under this condition [67]. The reduction states of cytochromes $b_{l/h}$, *c*, and aa_3 were measured in isolated pulmonary artery smooth muscle cells under normoxia and hypoxia [68]. Under hypoxia, cytochrome *c* and cytochrome aa_3 were reduced, whereas cytochrome $b_{l/h}$ was oxidized. This is in a good agreement with a mechanism of ubiquinol oxidation by complex III [27] and suggests that the Q pool stays nearly fully reduced as it cannot be oxidized by complex III because of the lack of oxidized cytochrome *c*. Interestingly, under the hypoxia condition, higher rates of mitochondrial superoxide production were observed using the superoxide-sensitive dye MitoSOX [68]. Therefore, our novel in vitro findings can provide a firm foundation for future investigations of site-specific ROS production in muscle under physiological conditions (e.g., rest vs exercise) and in diseases featuring altered lipid metabolism.

Acknowledgments

This work was supported by National Institutes of Health Grants R01 AG033542 and TL1 AG032116 and by The Ellison Medical Foundation, Grant AG-SS-2288-09.

Abbreviations

PC	palmitoylcarnitine
ETF	electron-transferring flavoprotein
ETFQOR	electron-transferring flavoprotein ubiquinone oxidoreductase
Q	ubiquinone
QH_2	ubiquinol
ROS	reactive oxygen species
Site I_F	flavin site of complex I
Site I_Q	ubiquinone-binding site of complex I
Site II_F	flavin site of complex II
Site III_{Qo}	outer ubiquinone-binding site of complex III
GPDH	glycerol 3-phosphate dehydrogenase
SOD	superoxide dismutase
DCPIP	dichlorophenolindophenol
FCCP	carbonyl cyanide 4-(trifluoromethoxy)phenylhydrazone
CDNB	1-chloro-2,4-dinitrobenzene

References

1. Romijn JA, Coyle EF, Sidossis LS, Gastaldelli A, Horowitz JF, Endert E, et al. Regulation of endogenous fat and carbohydrate metabolism in relation to exercise intensity and duration. Am J Physiol. 1993; 265:E380–E391. [PubMed: 8214047]
2. Hoppeler H. Skeletal muscle substrate metabolism. Int J Obes Relat Metab Disord. 1999; 23(Suppl 3):S7–10. [PubMed: 10367997]
3. Laforet P, Vianey-Saban C. Disorders of muscle lipid metabolism: diagnostic and therapeutic challenges. Neuromuscul Disord. 2010; 20:693–700. [PubMed: 20691590]
4. Rodrigues JV, Gomes CM. Mechanism of superoxide and hydrogen peroxide generation by human electron-transfer flavoprotein and pathological variants. Free Radic Biol Med. 2012; 53:12–19. [PubMed: 22588007]
5. Houstis N, Rosen ED, Lander ES. Reactive oxygen species have a causal role in multiple forms of insulin resistance. Nature. 2006; 440:944–948. [PubMed: 16612386]
6. Patti ME, Corvera S. The role of mitochondria in the pathogenesis of type 2 diabetes. Endocr Rev. 2010; 31:364–395. [PubMed: 20156986]
7. Lefort N, Glancy B, Bowen B, Willis WT, Bailowitz Z, De Filippis EA, et al. Increased reactive oxygen species production and lower abundance of complex I subunits and carnitine palmitoyltransferase 1B protein despite normal mitochondrial respiration in insulin-resistant human skeletal muscle. Diabetes. 2010; 59:2444–2452. [PubMed: 20682693]
8. Koves TR, Ussher JR, Noland RC, Slentz D, Mosedale M, Ilkayeva O, et al. Mitochondrial overload and incomplete fatty acid oxidation contribute to skeletal muscle insulin resistance. Cell Metab. 2008; 7:45–56. [PubMed: 18177724]
9. Kim JJ, Battaile KP. Burning fat: the structural basis of fatty acid beta-oxidation. Curr Opin Struct Biol. 2002; 12:721–728. [PubMed: 12504675]
10. Mackenzie J, Pedersen L, Arent S, Henriksen A. Controlling electron transfer in acyl-CoA oxidases and dehydrogenases: a structural view. J Biol Chem. 2006; 281:31012–31020. [PubMed: 16887802]
11. Ruzicka FJ, Beinert H. A new iron–sulfur flavoprotein of the respiratory chain:a component of the fatty acid beta oxidation pathway. J Biol Chem. 1977; 252:8440–8445. [PubMed: 925004]
12. Ramsay RR, Steenkamp DJ, Husain M. Reactions of electron-transfer flavoprotein and electron-transfer flavoprotein: ubiquinone oxidoreductase. Biochem J. 1987; 241:883–892. [PubMed: 3593226]
13. Beckmann JD, Frerman FE. Electron-transfer flavoprotein–ubiquinone oxidoreductase from pig liver: purification and molecular, redox, and catalytic properties. Biochemistry. 1985; 24:3913–3921. [PubMed: 4052375]
14. Starkov AA. The role of mitochondria in reactive oxygen species metabolism and signaling. Ann N Y Acad Sci. 2008; 1147:37–52. [PubMed: 19076429]
15. Murphy MP. How mitochondria produce reactive oxygen species. Biochem J. 2009; 417:1–13. [PubMed: 19061483]
16. Brand MD. The sites and topology of mitochondrial superoxide production. Exp Gerontol. 2010; 45:466–472. [PubMed: 20064600]
17. Quinlan CL, Orr AL, Perevoshchikova IV, Treberg JR, Ackrell BA, Brand MD. Mitochondrial complex II can generate reactive oxygen species at high rates in both the forward and reverse reactions. J Biol Chem. 2012; 287:27255–-27264. [PubMed: 22689576]
18. Orr AL, Quinlan CL, Perevoshchikova IV, Brand MD. A refined analysis of superoxide production by mitochondrial sn-glycerol 3-phosphate dehydrogenase. J Biol Chem. 2012; 287:42921–42935. [PubMed: 23124204]
19. Quinlan CL, Treberg JR, Perevoshchikova IV, Orr AL, Brand MD. Native rates of superoxide production from multiple sites in isolated mitochondria measured using endogenous reporters. Free Radic Biol Med. 2012; 53:1807–1817. [PubMed: 22940066]
20. St-Pierre J, Buckingham JA, Roebuck SJ, Brand MD. Topology of superoxide production from different sites in the mitochondrial electron transport chain. J Biol Chem. 2002; 277:44784–44790. [PubMed: 12237311]

21. Lambert AJ, Brand MD. Superoxide production by NADH:ubiquinone oxidoreductase (complex I) depends on the pH gradient across the mitochondrial inner membrane. Biochem J. 2004; 382:511–517. [PubMed: 15175007]
22. Tahara EB, Navarete FD, Kowaltowski AJ. Tissue-, substrate-, and site-specific characteristics of mitochondrial reactive oxygen species generation. Free Radic Biol Med. 2009; 46:1283–1297. [PubMed: 19245829]
23. Hoffman DL, Brookes PS. Oxygen sensitivity of mitochondrial reactive oxygen species generation depends on metabolic conditions. J Biol Chem. 2009; 284:16236–16245. [PubMed: 19366681]
24. Seifert EL, Estey C, Xuan JY, Harper ME. Electron transport chain-dependent and -independent mechanisms of mitochondrial H_2O_2 emission during long-chain fatty acid oxidation. J Biol Chem. 2010; 285:5748–5758. [PubMed: 20032466]
25. Schonfeld P, Wojtczak L. Brown adipose tissue mitochondria oxidizing fatty acids generate high levels of reactive oxygen species irrespective of the uncoupling protein-1 activity state. Biochim Biophys Acta. 2012; 1817:410–418. [PubMed: 22226918]
26. Affourtit C, Quinlan CL, Brand MD. Measurement of proton leak and electron leak in isolated mitochondria. Methods Mol Biol. 2012; 810:165–182. [PubMed: 22057567]
27. Quinlan CL, Gerencser AA, Treberg JR, Brand MD. The mechanism of superoxide production by the antimycin-inhibited mitochondrial Q-cycle. J Biol Chem. 2011; 286:31361–31372. [PubMed: 21708945]
28. Treberg JR, Quinlan CL, Brand MD. Hydrogen peroxide efflux from muscle mitochondria underestimates matrix superoxide production—a correction using glutathione depletion. FEBS J. 2010; 277:2766–2778. [PubMed: 20491900]
29. Klingenberg M, Pette D. Proportions of mitochondrial enzymes and pyridine nucleotides. Biochem Biophys Res Commun. 1962; 7:430–432. [PubMed: 14457017]
30. Estabrook RW. Fluorometric measurement of reduced pyridine nucleotide in cellular and subcellular particles. Anal Biochem. 1962; 4:231–245. [PubMed: 13890836]
31. Crofts AR, Meinhardt SW, Jones KR, Snozzi M. The role of the quinone pool in the cyclic electron-transfer chain of *Rhodopseudomonas sphaeroides*: a modified Q-cycle mechanism. Biochim Biophys Acta. 1983; 723:202–218. [PubMed: 21494412]
32. Schulz H. Regulation of fatty acid oxidation in heart. J Nutr. 1994; 124:165–171. [PubMed: 8308565]
33. Marquis NR, Fritz IB. The distribution of carnitine, acetylcarnitine, and carnitine acetyltransferase in rat tissues. J Biol Chem. 1965; 240:2193–2196. [PubMed: 14299646]
34. Miyadera H, Shiomi K, Ui H, Yamaguchi Y, Masuma R, Tomoda H, et al. Atpenins, potent and specific inhibitors of mitochondrial complex II (succinate-ubiquinone oxidoreductase). Proc Natl Acad Sci USA. 2003; 100:473–477. [PubMed: 12515859]
35. Turrens JF, Alexandre A, Lehninger AL. Ubisemiquinone is the electron donor for superoxide formation by complex III of heart mitochondria. Arch Biochem Biophys. 1985; 237:408–414. [PubMed: 2983613]
36. Ksenzenko M, Konstantinov AA, Khomutov GB, Tikhonov AN, Ruuge EK. Effect of electron transfer inhibitors on superoxide generation in the cytochrome bc_1 site of the mitochondrial respiratory chain. FEBS Lett. 1983; 155:19–24. [PubMed: 6301880]
37. Starkov AA, Fiskum G. Myxothiazol induces H_2O_2 production from mitochondrial respiratory chain. Biochem Biophys Res Commun. 2001; 281:645–-650. [PubMed: 11237706]
38. Rydstrom J. Mitochondrial NADPH, transhydrogenase and disease. Biochim Biophys Acta. 2006; 1757:721–726. [PubMed: 16730324]
39. Hansford RG, Hogue BA, Mildaziene V. Dependence of H_2O_2 formation by rat heart mitochondria on substrate availability and donor age. J Bioenerg Biomembr. 1997; 29:89–95. [PubMed: 9067806]
40. Kushnareva Y, Murphy AN, Andreyev A. Complex I-mediated reactive oxygen species generation: modulation by cytochrome c and $NAD(P)^+$ oxidation–reduction state. Biochem J. 2002; 368:545–553. [PubMed: 12180906]
41. Starkov AA, Fiskum G. Regulation of brain mitochondrial H_2O_2 production by membrane potential and NAD(P)H redox state. J Neurochem. 2003; 86:1101–1107. [PubMed: 12911618]

42. Treberg JR, Quinlan CL, Brand MD. Evidence for two sites of superoxide production by mitochondrial NADH-ubiquinone oxidoreductase (complex I). J Biol Chem. 2011; 286:27103–27110. [PubMed: 21659507]
43. Miwa S, St-Pierre J, Partridge L, Brand MD. Superoxide and hydrogen peroxide production by *Drosophila* mitochondria. Free Radic Biol Med. 2003; 35:938–948. [PubMed: 14556858]
44. Lambert AJ, Brand MD. Inhibitors of the quinone-binding site allow rapid superoxide production from mitochondrial NADH:ubiquinone oxidoreductase (complex I). J Biol Chem. 2004; 279:39414–39420. [PubMed: 15262965]
45. Schonfeld P, Wieckowski MR, Lebiedzinska M, Wojtczak L. Mitochondrial fatty acid oxidation and oxidative stress: lack of reverse electron transfer-associated production of reactive oxygen species. Biochim Biophys Acta. 2010; 1797:929–938. [PubMed: 20085746]
46. Boveris A, Cadenas E. Mitochondrial production of superoxide anions and its relationship to the antimycin insensitive respiration. FEBS Lett. 1975; 54:311–314. [PubMed: 236930]
47. Muller F, Crofts AR, Kramer DM. Multiple Q-cycle bypass reactions at the Q_o site of the cytochrome bc_1 complex. Biochemistry. 2002; 41:7866–7874. [PubMed: 12069575]
48. Voltti H, Hassinen IE. Oxidation–reduction midpoint potentials of mitochondrial flavoproteins and their intramitochondrial localization. J Bioenerg Biomembr. 1978; 10:45–58. [PubMed: 555461]
49. Kunz WS, Gellerich FN. Quantification of the content of fluorescent flavoproteins in mitochondria from liver, kidney cortex, skeletal muscle, and brain. Biochem Med Metab Biol. 1993; 50:103–110. [PubMed: 8373630]
50. Kunz WS, Kunz W. Contribution of different enzymes to flavoprotein fluorescence of isolated rat liver mitochondria. Biochim Biophys Acta. 1985; 841:237–246. [PubMed: 4027266]
51. Treberg JR, Brand MD. A model of the proton translocation mechanism of complex I. J Biol Chem. 2011; 286:17579–17584. [PubMed: 21454533]
52. Verkhovskaya ML, Belevich N, Euro L, Wikstrom M, Verkhovsky MI. Real-time electron transfer in respiratory complex I. Proc Natl Acad Sci USA. 2008; 105:3763–3767. [PubMed: 18316732]
53. Bonomi F, Pagani S, Cerletti P, Giori C. Modification of the thermodynamic properties of the electron-transferring groups in mitochondrial succinate dehydrogenase upon binding of succinate. Eur J Biochem. 1983; 134:439–445. [PubMed: 6884342]
54. Unden G, Bongaerts J. Alternative respiratory pathways of Escherichia coli: energetics and transcriptional regulation in response to electron acceptors. Biochim Biophys Acta. 1997; 1320:217–234. [PubMed: 9230919]
55. Barron JT, Gu L, Parrillo JE. NADH/NAD redox state of cytoplasmic glycolytic compartments in vascular smooth muscle. Am J Physiol Heart Circ Physiol. 2000; 279:H2872–H2878. [PubMed: 11087243]
56. Mohsen AW, Rigby SE, Jensen KF, Munro AW, Scrutton NS. Thermodynamic basis of electron transfer in dihydroorotate dehydrogenase B from *Lactococcus lactis*: analysis by potentiometry, EPR spectroscopy, and ENDOR spectroscopy. Biochemistry. 2004; 43:6498–6510. [PubMed: 15157083]
57. Zameitat E, Pierik AJ, Zocher K, Loffler M. Dihydroorotate dehydrogenase from *Saccharomyces cerevisiae*: spectroscopic investigations with the recombinant enzyme throw light on catalytic properties and metabolism of fumarate analogues. FEMS Yeast Res. 2007; 7:897–904. [PubMed: 17617217]
58. Paulsen KE, Orville AM, Frerman FE, Lipscomb JD, Stankovich MT. Redox properties of electron-transfer flavoprotein ubiquinone oxidoreductase as determined by EPR–spectroelectrochemistry. Biochemistry. 1992; 31:11755–11761. [PubMed: 1332770]
59. Usselman RJ, Fielding AJ, Frerman FE, Watmough NJ, Eaton GR, Eaton SS. Impact of mutations on the midpoint potential of the $[4Fe–4S]^{+1,+2}$ cluster and on catalytic activity in electron transfer flavoprotein-ubiquinone oxidoreductase (ETF-QO). Biochemistry. 2008; 47:92–100. [PubMed: 18069858]
60. Frerman FE. Reaction of electron-transfer flavoprotein ubiquinone oxidoreductase with the mitochondrial respiratory chain. Biochim Biophys Acta. 1987; 893:161–169. [PubMed: 3620453]
61. Wang R, Thorpe C. Reactivity of medium-chain acyl-CoA dehydrogenase toward molecular oxygen. Biochemistry. 1991; 30:7895–7901. [PubMed: 1868064]

62. Ghisla S, Thorpe C. Acyl-CoA dehydrogenases:a mechanistic overview. Eur J Biochem. 2004; 271:494–508. [PubMed: 14728676]

63. Simkovic M, Frerman FE. Alternative quinone substrates and inhibitors of human electron-transfer flavoprotein-ubiquinone oxidoreductase. Biochem J. 2004; 378:633–640. [PubMed: 14640977]

64. Hall CL, Lambeth JD. Studies on electron transfer from general acyl-CoA dehydrogenase to electron transfer flavoprotein. J Biol Chem. 1980; 255:3591–3595. [PubMed: 7364759]

65. Husain M, Stankovich MT, Fox BG. Measurement of the oxidation–reduction potentials for one-electron and two-electron reduction of electron-transfer flavoprotein from pig liver. Biochem J. 1984; 219:1043–1047. [PubMed: 6743239]

66. Zhang J, Frerman FE, Kim JJ. Structure of electron transfer flavoprotein-ubiquinone oxidoreductase and electron transfer to the mitochondrial ubiquinone pool. Proc Natl Acad Sci USA. 2006; 103:16212–16217. [PubMed: 17050691]

67. Liu MS, Siess M, Hoffmann PC. The effect of changes in functional activity on ubiquinone redox status in isolated atria. Eur J Biochem. 1973; 37:259–269. [PubMed: 4745731]

68. Sommer N, Pak O, Schorner S, Derfuss T, Krug A, Gnaiger E, et al. Mitochondrial cytochrome redox states and respiration in acute pulmonary oxygen sensing. Eur Respir J. 2010; 36:1056–1066. [PubMed: 20516051]

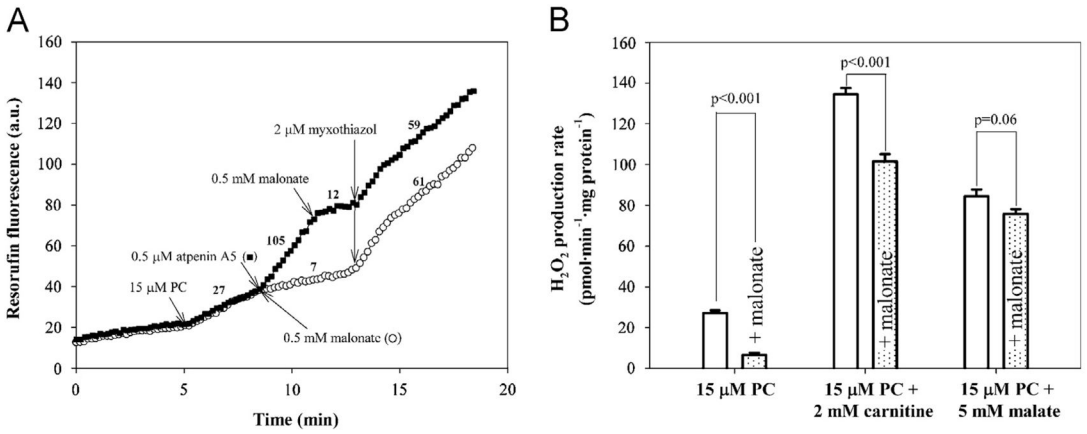

Fig. 1.

Effects of complex II inhibitors, malonate and atpenin A5, on rates of H_2O_2 production by rat skeletal muscle mitochondria oxidizing palmitoylcarnitine alone and in combination with carnitine or malate. (A) Typical traces of H_2O_2 production during palmitoylcarnitine oxidation and effects of complex II inhibitors. Palmitoylcarnitine (PC) was added after 5 min incubation of mitochondria (0.3 mg protein · ml^{-1}) with the Amplex UltraRed detection system plus exogenous SOD. The background rates in the absence of substrate were subtracted from all rates after substrate addition. Numbers by the traces represent rates of H_2O_2 production in pmol · min^{-1} · mg $protein^{-1}$ after calibration by addition of known amounts of H_2O_2. The addition of atpenin A5 increased the rate of H_2O_2 production during oxidation of palmitoylcarnitine from 27 ±1 (*n*=6) to 105±5 (*n*=4) pmol · min^{-1} · mg $protein^{-1}$. After addition of malonate it decreased to 7±1 pmol · min^{-1} · mg $protein^{-1}$ (*n*=4). Subsequent numbers are rates for the presented traces (*n*=1). (B) Effects of malonate addition on the rates of H_2O_2 production during oxidation of substrates from Table 1. Open bars, no malonate added; shaded bars, 0.5 mM malonate added after substrate. Values are means ± SEM. *n*=4 (PC ± malonate), *n*=6 (PC + carnitine ± malonate), *n*=5 (PC + malate ± malonate). *p* values were calculated using an unpaired Student *t* test.

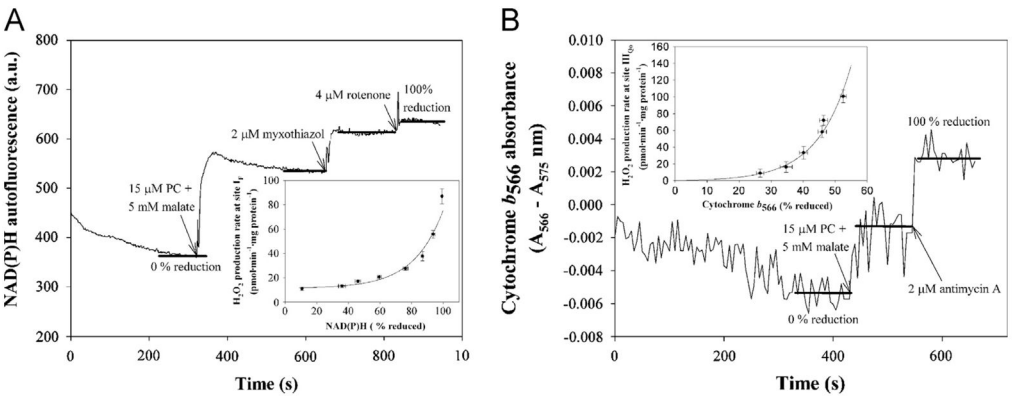

Fig. 2.

Reduction states of NAD(P) and cytochrome b_{566} as reporters of superoxide production from sites I_F (plus any other sites that respond to NADH reduction state) and III_{Qo}, respectively. Typical traces of (A) NAD(P)H autofluorescence and (B) cytochrome b_{566} absorbance in suspensions of skeletal muscle mitochondria (0.3 mg protein · ml^{-1} in (A) and 1.5 mg protein · ml^{-1} in (B)). The oxidized signal was established after 5 min incubation in the absence of substrates. Substrates were then added to establish the reduction state to be measured (in the example illustrated, 15 μM palmitoylcarnitine (PC) and 5 mM malate), followed by the addition of inhibitors (2 μM myxothiazol in (A)). 100% reduction was achieved by addition of 4 μM rotenone (A) or 2 μM antimycin A (B) in each run to calibrate the scale. 100% reduction in (B) was sometimes measured instead by adding 5 mM succinate plus 4 μM rotenone and 2 μM antimycin A and this value was used to calculate intermediate % reduction with other substrates during the experimental day. Insets are from [19]. Inset (A), calibration of the rate of H_2O_2 production at site I_F (pmol · min^{-1} · mg $protein^{-1}$) as a function of % reduction of NAD(P). Inset (B), calibration of the rate of H_2O_2 production at site III_{Qo}(pmol · min^{-1} · mg $protein^{-1}$) as a function of % reduction of cytochrome b_{566}.

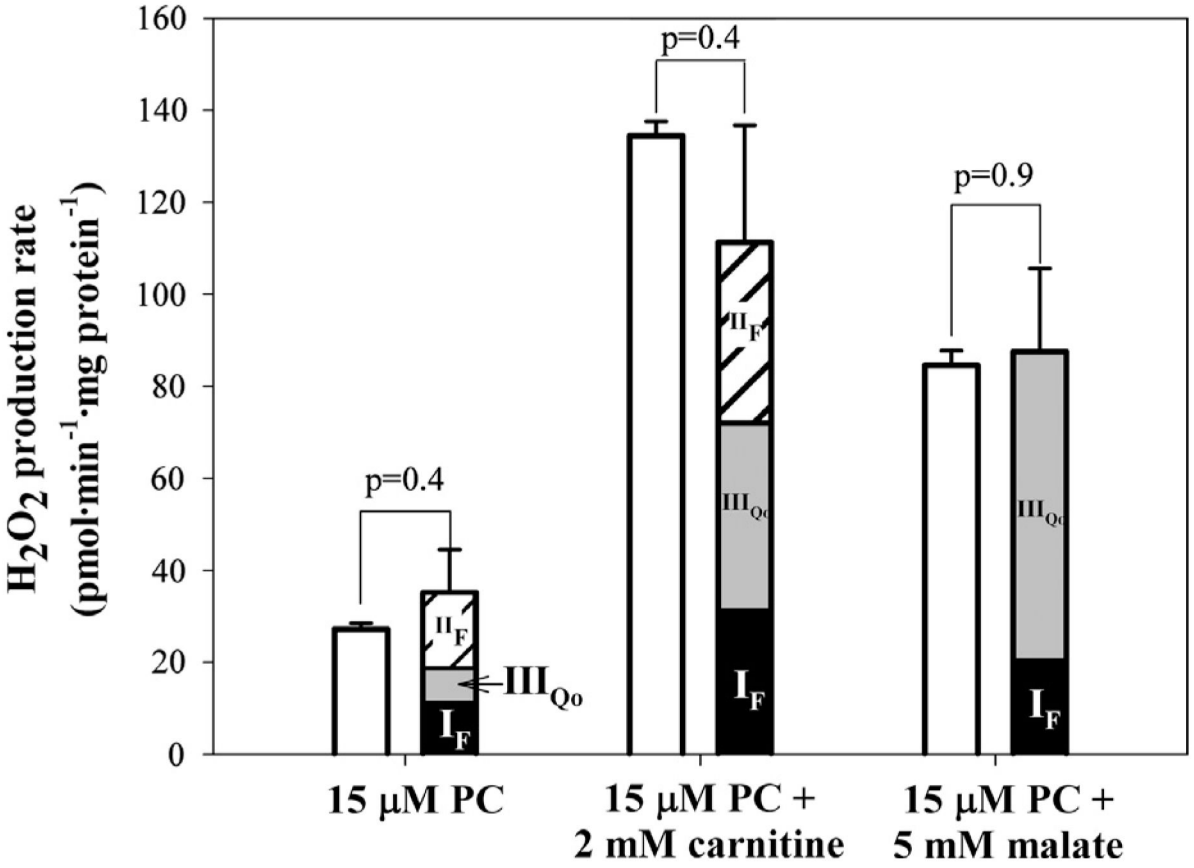

Fig. 3.

Comparison of the measured rate of H_2O_2 production and the sum of the predicted rates from sites I_F, II_F, and III_{Qo} under native conditions. Measured rates are from Fig. 1B and predicted rates are from Table 2. *p* values were determined by Welch's *t* test. The contribution of site II_F was corrected for changes at the other sites using the changes in the reduction states of NAD(P)$^+$ and cytochrome b_{566} upon addition of malonate. PC, palmitoylcarnitine.

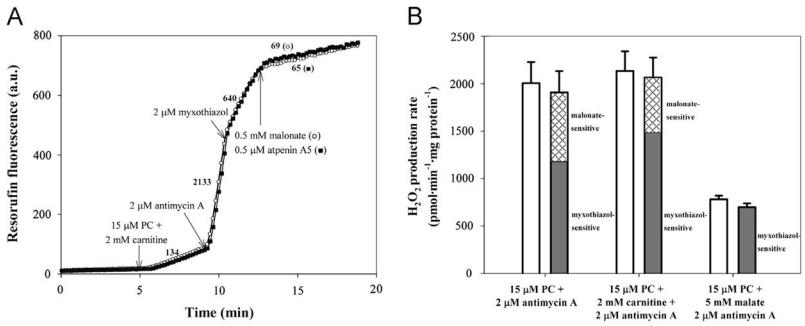

Fig. 4.

H_2O_2 production during oxidation of palmitoylcarnitine (PC) in the presence of the complex III_{Qi} inhibitor antimycin A. (A) Typical traces of H_2O_2 production during oxidation of palmitoylcarnitine plus carnitine and effects of inhibitors. Substrates and inhibitors were added as shown. Numbers by the traces represent rates of H_2O_2 production in pmol · min^{-1} · mg $protein^{-1}$ (*n*=6). (B) Total (open bars), myxothiazol-sensitive (gray bars), and malonate-sensitive (cross-hatched bars) rates of H_2O_2 production during oxidation of palmitoylcarnitine alone and in combination with carnitine or malate, all in the presence of antimycin A. Values are means ± SEM (*n*=6).

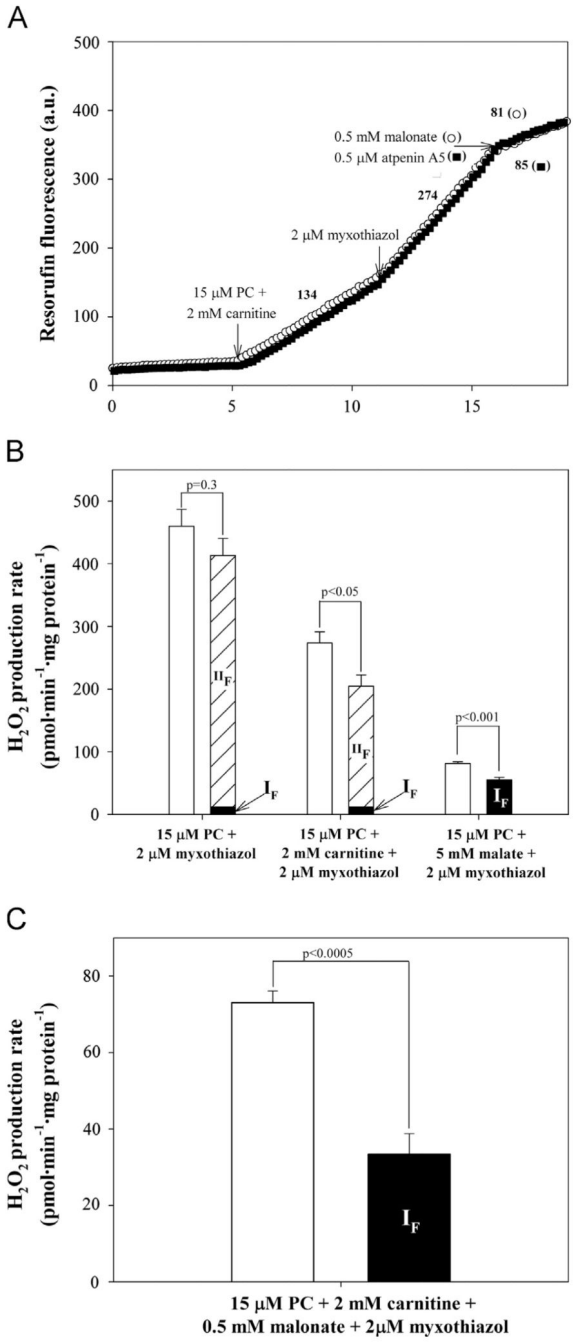

Fig. 5.

Measured and predicted rates of H_2O_2 production during oxidation of palmitoylcarnitine (PC) in the presence of the complex III_{Qo} inhibitor myxothiazol. (A) Typical traces of H_2O_2 production during oxidation of palmitoylcarnitine plus carnitine and effects of inhibitors. Substrates and inhibitors were added as shown. Numbers by the traces represent rates of H_2O_2 production in pmol · min^{-1} · mg $protein^{-1}$ (*n*=6). (B) Total measured rates of H_2O_2 production (open bars) and predicted rates from sites I_F (plus any other sites that respond to NADH reduction state) (black bars; predicted from the NAD(P) reduction state using the

calibration in Fig. 2A inset) and II_F (striped bars, predicted from the decrease in rate caused by addition of malonate after correction for changes in the predicted rate from site I_F after addition of malonate) during oxidation of palmitoylcarnitine alone and in combination with carnitine or malate, all in the presence of myxothiazol. Values are means ± SEM (n=6). p values were calculated by Welch's t test. (C) Total measured rates of H_2O_2 production (open bar) and predicted rates from site I_F (black bar; predicted as in (B)) during oxidation of palmitoylcarnitine alone and in combination with carnitine or malate, all in the presence of myxothiazol and malonate. Values are means ± SEM (n=6). p values were calculated by Welch's t test.

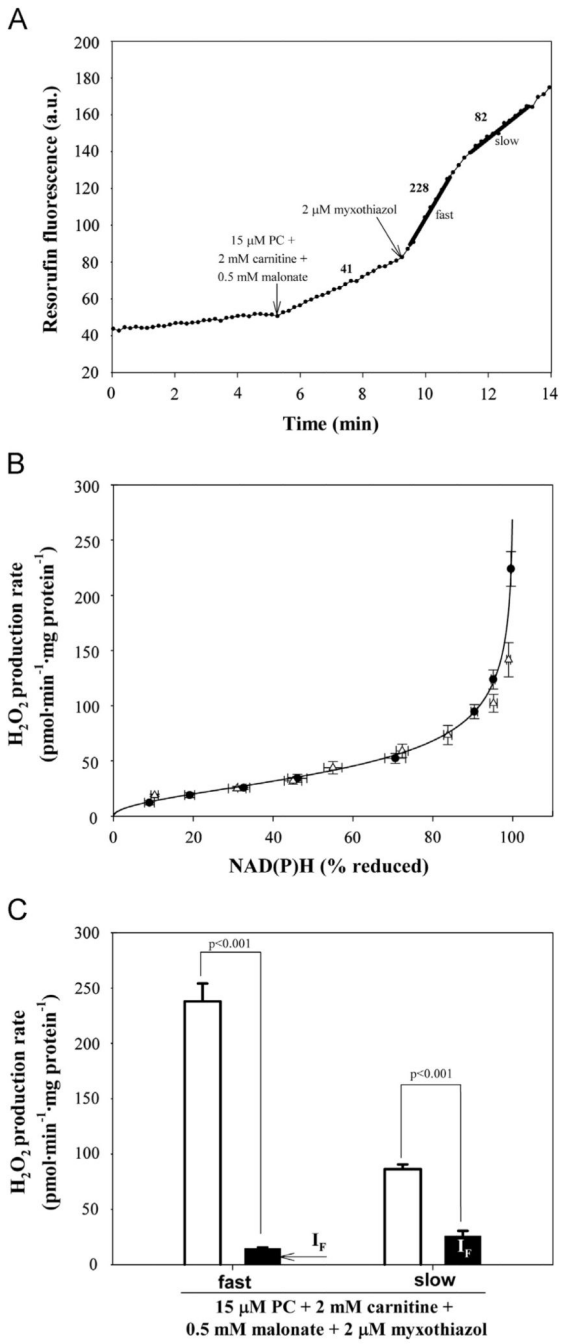

Fig. 6.

H_2O_2 production during oxidation of palmitoylcarnitine (PC) plus carnitine plus malonate in the presence of the uncoupler FCCP. (A) Typical trace of H_2O_2 production in the presence of 4 μM FCCP during oxidation of palmitoylcarnitine plus carnitine plus malonate and effect of addition of myxothiazol. The trace shows biphasic behavior: a first phase of high rate (labeled “fast”) and a second phase of slower rate (labeled “slow”). Numbers by the trace represent rates of H_2O_2 production in pmol · min^{-1} · mg $protein^{-1}$ (n=6). (B) Calibration of H_2O_2 production at site I_F (plus any other sites that respond to NADH reduction state) as a

function of reduction state of NAD(P)H in the presence of 4 μM FCCP (circles) (see Experimental procedures for details). The corresponding calibration in CDNB-treated mitochondria is also shown for comparison (triangles; data from [19]). (C) Total measured rates of H_2O_2 production (open bars) and predicted rates from site I_F (black bars; predicted using the calibration curve in (B)) during oxidation of palmitoylcarnitine plus carnitine, malonate, and myxothiazol. Values are means ± SEM (n=6). p values were calculated using Welch's t test.

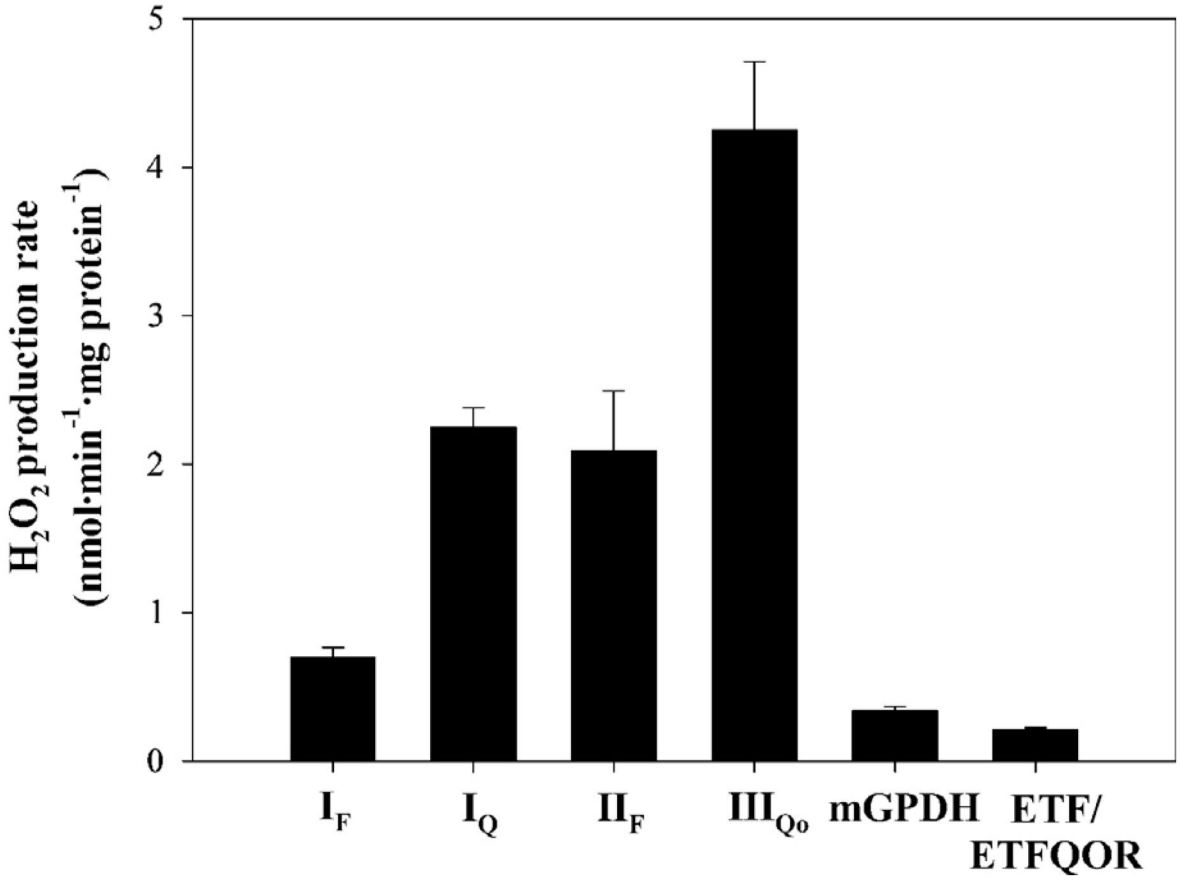

Fig. 7.

Maximum rates of H_2O_2 production from characterized sites of the mitochondrial respiratory chain. I_F, flavin site of complex I (plus any other sites that respond to NADH reduction state); I_Q, ubiquinone binding site of complex I; II_F, flavin site of complex II; III_{Qo}, Q_o binding site of complex III; mGPDH, mitochondrial glycerol 3-phosphate dehydrogenase; ETF/ETFQOR, electron-transferring flavoprotein/electron-transferring flavoprotein–ubiquinone oxidoreductase system. Data are from [19] except that for ETF/ETFQOR, which is from Fig. 6C.

Table 1

Oxygen consumption by rat skeletal muscle mitochondria.

Substrate	Oxygen consumption (nmol O · min^{-1} · mg $protein^{-1}$)			
	State 2	State 3	State 4_O	Uncoupled
5 mM succinate + 4 μM rotenone	133±14	654±39	212±18	478±24
15 μM palmitoylcarnitine	11±1	Unchanged	Unchanged	Unchanged
15 μM palmitoylcarnitine + 2 mM carnitine	57±6	96±15	72±8	100±15
15 μM palmitoylcarnitine + 5 mM malate	71±10	376±28	102±6	374±34

Mitochondria were incubated at 0.3 mg protein · ml^{-1} as described under Experimental procedures. State 2 respiration was measured after substrate addition. Subsequent additions were 0.5 mM ADP (to initiate State 3), 1 μg · ml^{-1} oligomycin (State 4_O), and 1 μM FCCP (uncoupled respiration). Values are means ±SEM for $n = 3$ independent experiments.

Table 2

Rates of H_2O_2 production from sites I_F (plus any other sites that respond to NADH reduction state), III_{Qo}, and II_F predicted from the reduction states of NAD(P)H and cytochrome b_{566} and the inhibition by malonate in rat skeletal muscle mitochondria with various substrate combinations.

Substrate	Site I_F		Site III_{Qo}		Site II_F corrected H_2O_2 (pmol · min^{-1} · mg $protein^{-1}$)
	NAD(P)H (% reduced)	H_2O_2 predicted (pmol · min^{-1} · mg $protein^{-1}$)	Cytochrome b_{566} (% reduced)	H_2O_2 predicted (pmol · min^{-1} · mg $protein^{-1}$)	
15 μM palmitoylcarnitine	15.1±0.7 (6)	11.9±1.4	26.1±2.4 (6)	7.8±5.4	15.5±7.5
15 μM palmitoylcarnitine + 2 mM carnitine	79.9±0.7 (6)	32.9±2.8	42.2±3.0 (6)	39.5±14.5	39.6±21.0
15 μM palmitoylcarnitine + 5 mM malate	65.7±1.4 (6)	21.3±1.8	47.5±2.3 (6)	66.2±18.0	
15 μM palmitoylcarnitine + 0.5 mM malonate	13.8±0.8 (5)	11.8±1.4	16.6±1.0 (4)	2.7±4.9	
15 μM palmitoylcarnitine + 2 mM carnitine + 0.5 mM malonate	79.3±1.1 (6)	32.2±2.8	43.8±2.4 (6)	46.2±14.4	

The reduction states of NAD(P) and cytochrome b_{566} were measured under the conditions of Figs. 1 and 2. The rates of H_2O_2 production from sites I_F and III_{Qo} were predicted from the calibration curves in Fig. 2A and B (insets). To calculate the corrected rates from site II_F, the measured decreases in H_2O_2 production rate caused by addition of malonate in Fig. 1B were corrected for the changes in rate from sites I_F and III_{Qo} predicted from the changes in reduction state of the endogenous reporters ± malonate. Values are means ± SEM (*n* independent experiments). The SEM of the predicted rates of H_2O_2 production from sites I_F and III_{Qo} were calculated by propagation of calibration and measurement errors using the equations in [19]. The SEM of the corrected rate from site II_F was calculated as $SEM = \sqrt{(SEM_a^2 + SEM_b^2 + SEM_c^2)}$, where SEM_a, SEM_b, and SEM_c represent the errors of the predicted rates from sites I_F and III_{Qo} before and after malonate addition and the SEM of the rate from site II_F assessed as the malonate-sensitive rate in Fig. 1B.

Free Radic Biol Med. Author manuscript; available in PMC 2014 October 11.